Agricultural and Forest Meteorology 151 (2011) 70–77

Contents lists available at ScienceDirect

Agricultural and Forest Meteorology

journal homepage: www.elsevier.com/locate/agrformet

Pressure correction to the long-term measurement of carbon dioxide flux

Junhui Zhang[a,*], Xuhui Lee[b], Guozheng Song[a], Shijie Han[a]

[a] Institute of Applied Ecology, Chinese Academy of Sciences, 72 Wenhua Road, Shenyang 110016, China
[b] School of Forestry and Environmental Studies, Yale University, New Haven 06511, USA

ARTICLE INFO

Article history:
Received 31 December 2009
Received in revised form 7 September 2010
Accepted 8 September 2010

Keywords:
Pressure term
Eddy-covariance
Long-term
CO_2 budget
Canopy density

ABSTRACT

Fluctuations in atmospheric CO_2 density can arise from static pressure fluctuations but their effect on the long-term eddy covariance (EC) CO_2 flux measurement is poorly known. In this paper, we report the results of a 1-year direct measurement of the static pressure fluctuations and the velocity–pressure covariance over a mixed forest in Northeast China. The results show that the pressure–vertical velocity covariance was primarily controlled by friction velocity and air stability. Without the pressure correction, the open-path EC measurement of the nighttime ecosystem respiration was biased low and that of the daytime photosynthetic CO_2 uptake was biased high. Over the 1-year measurement period, the cumulative pressure correction was 40 gCm^{-2}, which was about 20% of the annual net ecosystem production of this forest. Using the friction velocity data found in the literature, we estimated the magnitudes of the pressure correction for the major ecosystem types in the long-term global EC network (FluxNet).

1. Introduction

The eddy-covariance (EC) technique has been widely used to investigate the carbon budget of terrestrial ecosystems and their responses to environmental stresses (e. g. Baldocchi, 2003). It is a direct method to measure the carbon dioxide exchange at the ecosystem level with a high temporal resolution. A large body of literature is devoted to quantifying the uncertainties of the EC method for long-term measurement. Substantial effort has been made to establish the causes of the uncertainties, such as advection (Aubinet et al., 2003; Baldocchi et al., 2000; Lee, 1998; Lee and Hu, 2002; Paw U et al., 2000; Staebler and Fitzjarrald, 2004), descending motion associated with stationary convective cells (Lee et al., 1994), and drainage flow (Aubinet, 2008; Goulden et al., 2006; Grace et al., 1996). These studies demonstrate that the vertical eddy flux term alone in the CO_2 mass conservation equation is not enough to close the ecosystem CO_2 budget.

Another source of uncertainty arises from density effects on atmospheric CO_2. Traditionally, the net ecosystem CO_2 exchange (NEE) is obtained by integrating the xCO_2 conservation equation in the vertical direction. Accounting for the WPL density effects (Webb et al., 1980) and ignoring the advection terms, Massman and Lee (2002) showed that NEE is expressed as

$$\mathbf{NEE} = \int_0^{z_r} \frac{\partial \bar{\rho}_c}{\partial t} dz + \overline{w'\rho_c'} + \left[\delta_{oc}\bar{\rho}_c(1+\bar{\chi}_v)\frac{\overline{w'T_a'}}{\overline{T_a}} + \bar{\omega}_c\mu_v\overline{w'\rho_v'}\right] - \bar{\rho}_c(1+\bar{\chi}_v)\frac{\overline{w'p_a'}}{\bar{p}_a} \quad (1)$$

where the overbar denotes time averaging, prime denotes departure from the time average, ρ_c is the ambient CO_2 density, w is the vertical velocity, χ_v is the volume mixing ratio of water vapor, T_a is the ambient temperature, ω_c is the mass mixing ratio of CO_2, μ_v is the ratio of the molecular mass of dry air to that of water vapor, ρ_v is the ambient water vapor density, p_a is the ambient pressure, and $\delta_{oc} = 1$ for an open-path sensor and $\delta_{oc} = 0$ for a closed-path sensor. On the right-hand side of Eq. (1), the first term is the storage flux, the second term is the eddy flux, the third term is the traditional WPL correction term, the last term is the density correction arising from pressure fluctuations.

The pressure term, the last term on the right-hand side of Eq. (1), is usually omitted in EC studies. Massman and Lee (2002) suggested that this term can amount to as much as 5.1 $tC\,ha^{-1}\,yr^{-1}$, although their estimate may have overstated the severity of the problem as their pressure fluctuations were measured at an usually windy forest site. Using the function developed by Wilczak et al. (1999) over an ocean surface, Zhang et al. (2006a) showed that the correction to the CO_2 flux for the pressure fluctuations is on the order of 1–30% of the annual cumulative eddy flux. So far, no published study has reported the direct measurement of the pressure correction term over an annual cycle. Even though the pressure correction is smaller in magnitude than the correction for heat and

* Corresponding author. Fax: +86 24 8397 0300.
E-mail addresses: jhzhang@iae.ac.cn (J. Zhang), xuhui.lee@yale.edu (X. Lee).

0168-1923/$ – see front matter © 2010 Elsevier B.V. All rights reserved.
doi:10.1016/j.agrformet.2010.09.004

water vapor, the cumulative bias can be substantial because the pressure flux, $\overline{w'p'}$, is always in the same direction regardless of time of the day and season.

Static pressure fluctuations and air motion are intrinsically related. In the surface layer, the fluctuations usually increase with increasing wind speed (McBean and Elliott, 1975; Sigmon et al., 1983). The strength of the fluctuations depends on canopy height, with the p standard deviation varying from 0.05 to 0.2 Pa above a grass surface (Albertson et al., 1998), 0.5–3 Pa above a wheat canopy (Maitani and Seo, 1985), and 1–7 Pa above forests (Sigmon et al., 1983). Significant fluctuations of static pressure are thought to be related to the passage of coherent structures in near-neutral to convective conditions (Gao et al., 1992; Shaw et al., 1990; Zhuang and Amiro, 1994) and to the presence of gravity waves in stable conditions (Lee, 1997).

Pressure is the least investigated basic variable in micrometeorology. Of the few studies cited above, some rely on direct observations of high frequency p time series and others infer the variations from the momentum equations. They are limited to a narrow range of stability conditions and short measurement campaigns. Questions still remain as to how the pressure flux varies according to stability, surface roughness and vegetation morphology.

In this paper, we report the results of a 1-year direct measurement of the static pressure fluctuations and the velocity–pressure covariance over a mixed forest in Northeast China. Our specific objectives are (1) to explore the influences of canopy density and air stability on the pressure fluctuations and the pressure flux, (2) to evaluate the contribution of the pressure term to the annual CO_2 budget, and (3) to estimate the annual NEE bias errors associated with the pressure term for other terrestrial ecosystems in the long-term eddy covariance flux network.

2. Material and methods

2.1. Site and routine EC measurement

The experiment was carried out at Plot 1 in the Forest Ecosystem Open Research Station of Changbai Mountains (128.828°E and 42.824°N), Chinese Academy of Sciences, from April 2007 to June 2008. The maximum fetch of 60 km was found in the E–S–W directions and a minimum of 500 m in the NE direction. The dominant wind direction was SW. The annual mean temperature was 2.6 °C and the mean precipitation was 674 mm yr^{-1} over the period 1959–2005. The area surrounding the site was covered by a mixed forest consisting of over 200 uneven-aged species including Korean pine (*Pinus koraiensis*), Amur linden (*Tilia amurensis*), Mono maple (*Acer mono*), Manchurian ash (*Fraxinus mandshurica*) and Mongolian oak (*Quercus mongolica*). The mean canopy height was 26 m. A dense understory, consisting of broad-leaved shrubs, was 0.5–2 m tall. The peak leaf area index (LAI) was about 6.1. The LAI in the dormant season was about 2.1. The terrain slope was less than 2°.

Flux observations at this site have continued since 2002 (Zhang et al., 2006a,b). An EC system was installed at the height of 40 m above the ground on a 62.8 m tower. CO_2, H_2O, wind and temperature fluctuations were measured with an open-path CO_2/H_2O sensor (model Li7500, Li-Cor, USA) and a 3D ultrasonic anemometer (model CSAT3, Campbell Scientific, USA) at a rate of 10 Hz. Supporting meteorological variables were sampled every 2 s and stored as half-hourly statistics on a datalogger (model CR23X, Campbell Scientific, USA); They included air temperature and relative humidity (model HMP45C, Vaisala, Finland), wind speed (model A100R, Vector, UK), downward/upward solar radiation and net radiation (model CNR1, Kipp and Zonen, The Netherlands), barometric pressure (model CS105, Campbell Scientific, USA) and PAR (model Li190SB, Li-Cor, USA) at the 40-m height, and precipitation (model 52203, Young, USA) at the height of 62.8 m. Routine QA/QC procedures, such as coordinate rotation and correction for the density effects due to heat and water vapor exchange, were applied to the eddy flux data.

2.2. Pressure–velocity measurement

Fig. 1 is the diagram of the velocity–pressure measurement system. The probe consisted of two parallel flat disks with a pair of openings facing each other on the inner surface of the disks. The openings were connected to a highly sensitive differential pressure transducer (model 590 Barocel, Edwards High Vacuum International, USA) through a 65-cm long tube (type Dekoron 1300, Saint-Gobain Performance Plastics, USA, tube ID 0.64 cm). The pressure probe was constructed after the design by Robertson (1972) and Conklin (1994). This design is insensitive to wind direction and is able to eliminate the dynamic pressure contamination within a reasonable range of vertical angle of ±20° (Conklin, 1994). The reference port of the transducer was connected to a stainless steel 1 L flask which was bled to the ambient air via a capillary tube (37 cm long, 0.02 cm inner diameter). The turnover time of the air in the flask with the capillary tube was about 30 min. In the interest of

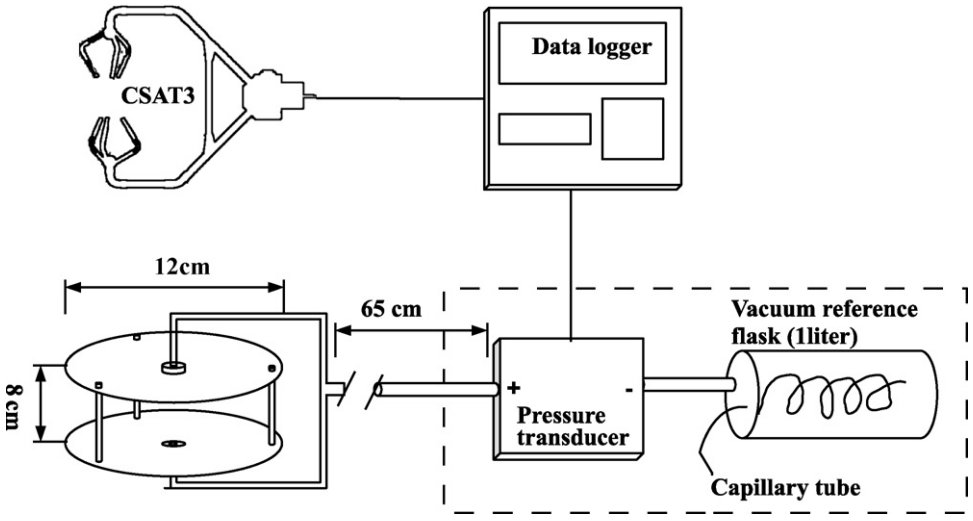

Fig. 1. Diagram showing the system for measuring wind velocity and static pressure fluctuations.

obtaining a stable performance, the transducer was mounted on a thermal base (model 525B, Edwards High Vacuum International, USA) and kept, together with the reference flask, in a thermally insulated wooden box. Once a week, the probe was checked and its level adjusted when necessary.

A 3D sonic anemometer (model CSAT3, Campbell Scientific, USA), independent of the routine EC system, was used with the pressure sensor to measure the pressure flux. The sonic anemometer was placed at 0.6 m directly above the pressure probe. Their signals were sampled and archived at 10 Hz by a datalogger (model CR5000, Campbell Scientific, USA). The pressure–velocity system was installed at the 40-m height, about 1.5 m away from the routine EC system. Both systems were directed toward the SW direction, the dominant wind direction at this site.

2.3. Data analysis

The data was calibrated against the curve developed by Conklin (1994) using a 1.5 m square cross section, laminar flow wind tunnel at the EPA Fluid Modeling Facility in Research Triangle Park, North Carolina. The pressure probe was built after the design by Robertson (1972) and Conklin (1994). The probe shows a flat response range of ±20°. Outside of the flat response region, the probe underestimates the pressure values. The response function seems to be independent of wind speed.

The pressure–velocity data were split into 30-min blocks to match the routine CO_2 flux calculation. Statistics were calculated after coordinate rotation into the natural wind system (Kaimal and Finnigan, 1994). Observations made within 4 h after the end of power outage and during precipitation events were not used for this analysis. Also excluded from the analysis were data collected when the wind direction was beyond ±45° of the dominant direction. The data points were treated as missing value when the vertical attack angle was larger than 20°. The observations were excluded from our analysis if the number of missing values and spikes was greater than 1% of the total number of data points within each 30-min. This procedure removed around 30% of the observations.

In addition to covariance statistics, power spectrum, phase spectrum and cospectrum were calculated with the continuous wavelet transformation (CWT) method. CWT is an ideal choice to produce unbiased estimate of spectra avoiding the limitation of the discrete wavelet transform and the fast Fourier transform (Foufoula-Georgiou and Kumar, 1994; Maraun, 2006). All the calculations were performed in the R environment (R Development Core Team, 2009).

3. Results and discussion

3.1. Pressure spectrum

Fig. 2 shows the ensemble p power spectrum grouped by atmospheric stability and season. The stability parameter ζ is defined as

$$\zeta = \frac{(z-d)}{L}$$

where z is the measurement height, d is displacement and L is the Monin–Obukhov length. Each ensemble spectrum represents the average of 200–600 30-min observations. The spectrum was scaled by the pressure standard deviation, σ_p, which had an average value of 1.84 Pa over the whole experimental period. The difference between the winter and summer season was very small, suggesting that the spectral distribution of the p fluctuations was insensitive to LAI (Fig. 3). This agrees with the study of Kimball and Lemon (1970). Their spectrum does not show the effect of the development of corn canopy on the shape of the pressure spectrum.

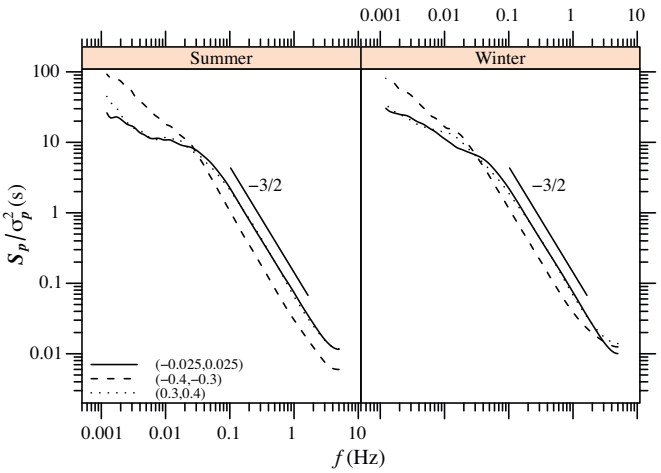

Fig. 2. Ensemble average spectrum grouped by stability parameter ζ and season. Values in the parentheses denote the ζ range.

The power spectrum follows the −3/2 slope in the inertial subrange for all the three stability classes. The magnitude of this slope is closer to the lower end of the range of values found in the literature. Elliott (1972) and Albertson et al. (1998) found a −5/3 and −3/2 slope, respectively, over grassland ecosystems. Kimball and Lemon (1970) and Sigmon et al. (1983) reported a slope of −2 over a corn canopy and within a deciduous forest, respectively. The work of Maitani and Seo (1985) over a wheat field indicates a slope of −7/3, which is suggested by the extension of the Kolmogorov scaling argument to the static pressure.

Several explanations exist for the variations in the spectrum slope. First, air flow over a forest canopy is different from the smooth-wall flow and the free-air flow. The roughness of the forest canopy shifts the pressure fluctuations to higher frequencies, thus decreasing the magnitude of the power slope. Evidence of this frequency shift can be found in the wind tunnel simulation by Blake (1970). Additionally, Albertson et al. (1998) argued that the interaction between large and small scale eddies should result in the −3/2 power slope. In the forest environment, these large eddies are essentially the coherent structures that dominate the transport of scalars and momentum (Barthlott et al., 2007; Gao et al., 1992; Lu and Fitzjarrald, 1994; Mahrt and Gibson, 1992; Raupach et al., 1996; Shaw et al., 1990; Thomas and Foken, 2007; Zhuang and Amiro, 1994). Second, the −7/3 power slope may be valid only for mesoscale motions whose frequencies are lower that the frequency range shown in Fig. 2. The reader should be aware that because the pressure transducer was operated in differential mode, the measured p time series was equivalent to a high-passed signal with the frequency cutoff roughly equal to the inverse of the turnover time of the sensor buffer volume, or 3×10^{-4} Hz. Canavero and Einaudi (1987) found that the pressure spectrum follows the −7/3 predic-

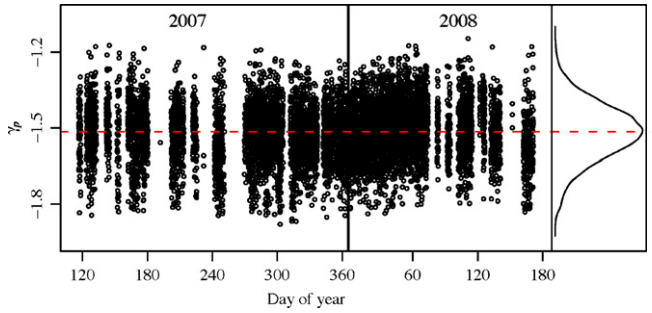

Fig. 3. Time course of the pressure spectrum slope in the inertial subrange.

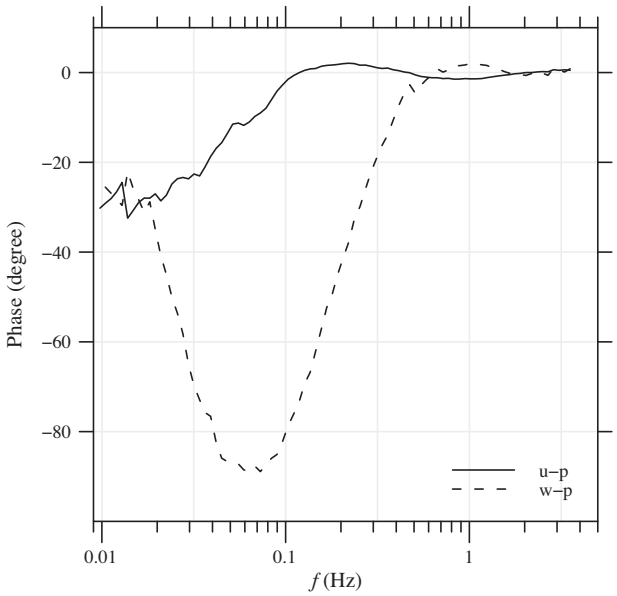

Fig. 4. Phase difference between pressure and velocity, estimated with data from DOY 180–200 in 2007.

tion in the frequency range of 1.95×10^{-4} Hz to 4.8810^{-5} Hz. Direct numerical simulations also show that two inertial subranges exist in the pressure spectrum, the first one being the classical −7/3 range corresponding to mesoscale motions and the second being the −5/3 range corresponding to isotropic turbulence at smaller scales (Gotoh and Rogallo, 1999).

Even though it was insensitive to LAI, the power spectrum was influenced by air stability and other factors. In Fig. 2, the spectrum in stable stratification was almost identical to that in neutral stability. The spectrum in unstable conditions shifted slightly to lower frequencies in comparison to the spectrum in stable and neutral conditions. Our study appears to be the first to report the stability-dependent behavior of the p spectrum. Sigmon et al. (1983) and Grachev and Mordukhovich (1988) found that the power slope of the pressure spectrum decreases with increasing of wind speed. Canavero and Einaudi (1987) reported a clear daily pattern in the power slope, possibly caused by the change in air stability.

The seasonality in the power slope was not detectable in Fig. 3, where the inertial subrange slope was evaluated for every 30-min observation and plotted over the annual cycle. The slope values followed a normal distribution centered at a mean value of 1.52.

The contamination of the p measurement by dynamic pressure fluctuations should have been very small. This is because the dynamic pressure fluctuations would have an equal and opposite effect on the two ports facing each other (Fig. 1). It is known that a phase of −180° exists between the horizontal velocity u and the dynamic pressure (McBean and Elliott, 1978). The observed phase difference in the u–p relationship was greater −40° (Fig. 4). The observed w–p phase did not agree with the behavior expected for the dynamic pressure which should exhibit roughly +90° phase with w. Using a large eddy simulation, Fitzmaurice et al. (2004) showed that in the roughness sublayer that the static pressure perturbations are more or less in phase with the u fluctuations. That the measured p fluctuations were within 40° in phase with u is an additional piece of evidence that the pressure probe was measuring the fluctuations of static pressure rather than dynamic pressure.

3.2. Covariance of atmospheric pressure and vertical velocity

The phase spectrum indicates that w and p were in general negatively correlated (Fig. 4). The pressure and vertical velocity

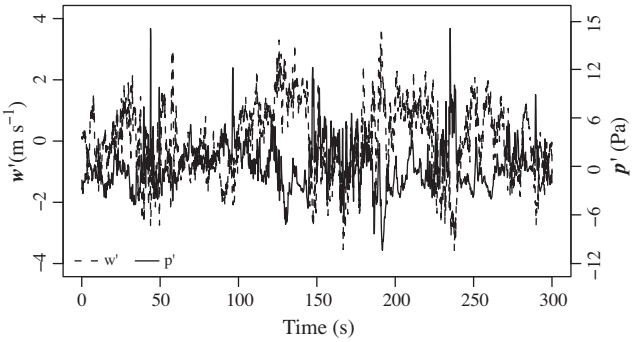

Fig. 5. A typical time series of the static pressure and vertical velocity fluctuations. The observation was made from 08:15 to 08:20 DOY 113, 2007.

fluctuations were approximately in phase for frequencies $f > 0.6$ Hz where the phase difference varied around zero. The pressure fluctuations led the vertical velocity at frequencies $f < 0.6$ Hz. The phase of −89° occurred at 0.07 Hz, the approximate peak frequency of the w–p cospectrum.

The negative w-p correlation is further illustrated with a time series plot in Fig. 5. An downward moving air parcel would cause a rise in the static pressure, and vice versa. The peak-to-peak p variation was about 20 Pa. The negative correlation indicates that the pressure flux $\overline{w'p'}$ was generally negative. In other words, turbulent motion resulted in a downward transport of the pressure force in the surface layer above the forest.

Fig. 6 shows the ensemble w–p cospectrum for three stability classes and two different seasons. The cospectrum was normalized by the total w–p covariance. The unnormalized cospectrum was negative at almost all the frequencies. For each stability class, the conspectrum shape and the peak frequency were broadly similar between the winter and the summer season. Under stable and neural conditions, the contribution by low-frequency eddies was slightly higher in the winter than in the summer: an ogive analysis (Berger et al., 2001) indicates that the contribution to the w–p covariance by scales $f > 0.01$ Hz was 80% in the winter and 90% in the summer.

The cospectrum appears to depend on stability. It was narrower and had a higher peak frequency (0.030 and 0.036 Hz for summer and winter, respectively) in neutral stability than in stable conditions (peak frequency 0.015 and 0.014 Hz for summer and winter, respectively). The cospectrum in unstable conditions shows a very broad peak between 0.002 and 0.02 Hz. The time scales corresponding to the peak frequencies fell in the range of 30–70 s under

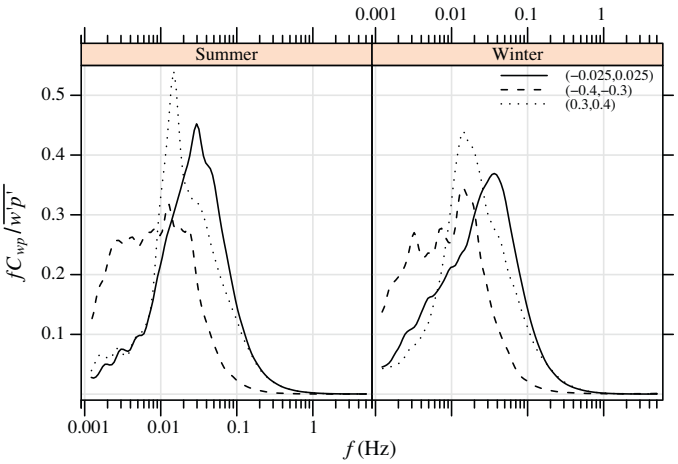

Fig. 6. Same as in Fig. 2 except for the w–p cospectrum.

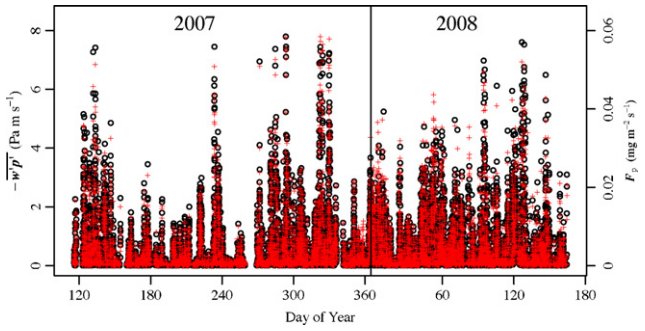

Fig. 7. Time courses of the pressure flux ($\overline{w'p'}$, ○) and the pressure correction term (F_p,+).

the three stratification groups except for the upper bound of the unstable stratification case. These time scales matched the average duration time of the coherent structures observed over forest (e.g. Lu and Fitzjarrald, 1994). It seems that pressure transport was dominated by these canopy-scale coherent eddies under both neutral and stratified conditions.

The seasonal course of the pressure flux is shown in Fig. 7. Over the experimental period, $\overline{w'p'}$ varied in the range −8 to 0 Pa m s^{-1}. The mean value was −0.61 Pa m s^{-1}. The flux was, on average, smaller in magnitude in the summer (mean value −0.38 Pa m s^{-1} from DOY 151–270) than in the winter (mean value −0.59 Pa m s^{-1} from DOY 301 in 2007 to 90 in 2008). This pattern followed the seasonal variation in wind speed.

According to the Monin–Obukhov similarity theory, the pressure flux $\overline{w'p'}$ scaled by $\rho_a u_*^3$ should be a universal function of the stability parameter ζ (McBean and Elliott, 1975), where ρ_a is air density and u_* is friction velocity. The ζ value varied from −9 to 7 during the experiment. The analysis presented below was restricted to the range $-1.5 < \zeta < 1.5$ that included 90% of the data. Beyond this range, the data points were few and scattered. The relationship was evaluated by season and with the whole dataset and was compared with several published relationships. For clarity, variables were bin-averaged with the standard error given as error bars.

The seasonality or LAI influence was discernible except in neutral conditions. The normalized pressure flux was about −2.0 at nuetral stability and increased in magnitude as ζ departed from zero. For comparison, the neutral stability value is approximately −2 over sea waves (Wilczak et al., 1999) and a forest canopy (Massman and Lee, 2002), −0.2 over a grassland (McBean and Elliott, 1975) and −0.02 from the static pressure fluctuations retrieved from the momentum and continuity equations in the convective boundary layer (Wilczak and Businger, 1984).

The following relationship was used to describe the observed pattern shown in Fig. 8,

$$F = \begin{cases} a_1\zeta + b_1, & -1.0 \le \zeta \le 0.0 \\ b_1, & 0.0 \le \zeta \le d \\ a_2\zeta + b_2, & d \le \zeta \le 1.0 \end{cases} \quad (2)$$

where $F = \overline{w'p'}/\rho_a u_*^3$ and a_1, a_2, b_1 and b_2 are regression coefficients. These coefficients were determined with a segmented linear regression method (Muggeo, 2003). To see the influence of canopy density, we evaluated F with the seasonal data and the whole dataset. The result is shown in Table 1. The slope parameter is 2.64 for the whole dataset in unstable conditions, slightly larger than the value of 2.3 reported for a grassland (McBean and Elliott, 1975) and smaller than 5.0 measured over sea waves (Wilczak et al., 1999).

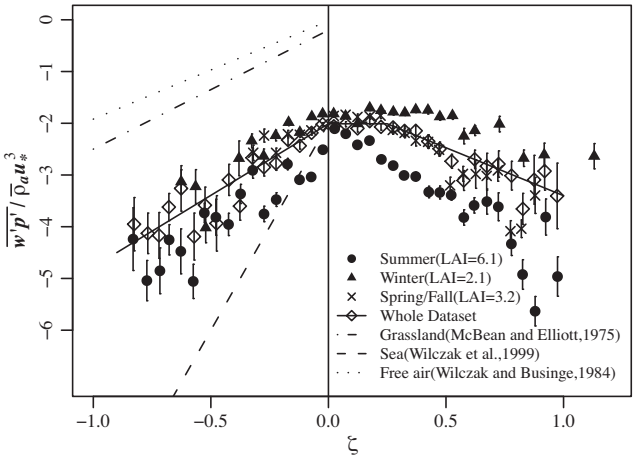

Fig. 8. Dependence of $\overline{w'p'}$ on air stability, grouped by season.

Table 1
Regressed parameters in Eq. (2).

Seasons[a]	a_1	b_1	a_2	b_2	d
Winter	2.99	−1.87	−1.38	−1.18	0.50
Spring/fall	2.22	−1.92	−2.91	−1.34	0.20
Summer	2.92	−2.13	−2.89	−1.84	0.10
Whole dataset	2.64	−2.01	−1.81	−1.56	0.25

[a] Winter DOY 301–365 and DOY 1–90; Spring: DOY 91–150; Fall: DOY 271–300; Summer: DOY 151–270.

3.3. Pressure correction to the eddy covariance carbon dioxide flux

The density correction for pressure fluctuations, given by the last term on the right side of Eq. (1), is

$$F_p = \frac{-\overline{\rho_c}(1+\overline{\chi_v})\overline{w'p'}}{\overline{p_a}} \quad (3)$$

This correction term varied from nearly zero to 0.06 mg m^2 s^{-1} throughout the year (Fig. 7), was generally higher in the winter than in the summer and higher in the day than at night (Fig. 9). Much of the variation in F_p was controlled by the variation in u^* (e.g.,

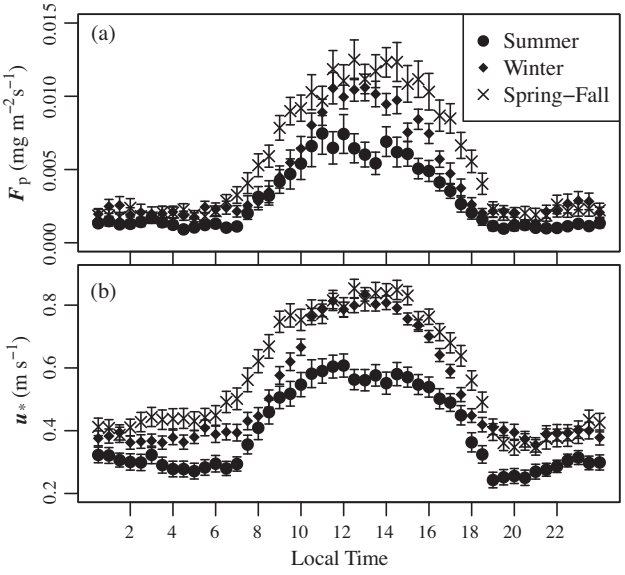

Fig. 9. Ensemble average diurnal course of the pressure correction (F_p, a) and friction velocity (u_*, b).

Fig. 9). Without the correction, the EC method would underestimate the nighttime ecosystem respiration and overestimate the daytime photosynthetic carbon uptake.

In comparison, the pressure fluctuations have no impact on sensible heat flux. Their role in the measurement of evapotranspiration is limited: A pressure flux of $-0.6\,\mathrm{Pa\,m\,s^{-1}}$ amounts to a correction of $0.0001\,\mathrm{g\,m^{-2}\,s^{-1}}$ or about 0.1% of a typical midday evapotranspiration rate. Similar assessment can be made for other scalars such as ozone and methane using Eq. (3).

To assess the impact of the pressure term on the annual NEE, we filled gaps in the pressure data with the formula developed above when the supporting measurements were available and with the linear interpolation or the mean daily variation method when otherwise. The cumulative F_P over the full annual cycle (DOY 180 in 2007 to DOY 180 in 2008) was $40\,\mathrm{g\,C\,m^2\,yr^{-1}}$, which is about 20% of the cumulative C flux of the same period. In other words, without the correction, the EC method would overestimate the annual net ecosystem production by $40\,\mathrm{g\,C\,m^2\,yr^{-1}}$. The density effect arising from the pressure flucations was clearly not negligible.

To obtain a rough estimate of how the pressure term may have biased the NEE data for other ecosystems, we surveyed the published literature (Appendix A) for information on u^*. A total of 44 studies were compiled, covering evergreen needleleaf forests (ENF), evergreen broadleaf forests (EBF), deciduous broadleaf forests (DBF), mixed forests (MF) and grassland (GRA). The annual mean correction flux was firstly calculated as

$$F_{p,1} = -\frac{\overline{\rho_c \rho_a F}}{\overline{p_a}}(1+\overline{\chi_v})\overline{u_*^3} \tag{4}$$

For ENF, EBF, DBF and MF, F was assigned two different values (-2 and -4) representing approximately the upper and lower bounds of the observations in our forest (Fig. 8). For GRA, F was assigned values of -0.2 and -2 according to McBean and Elliott (1975). The data reported in these studies, in the form the nighttime CO_2 flux as a function of u_*, were digitized into several u_* bins with the frequency in each bin noted. The temporal averaging operation in the above equation was approximated by weighting the u_*^3 value in each bin according to the frequency of occurrence in the bin.

Next, a correction factor, termed friction velocity pattern factor, was applied to Eq. (4) to account for the diurnal variations in u_*. This pattern factor was determined with the half-hourly observations at this forest and at a mixed forest in Connecticut, USA (Lee and Hu, 2002) in a two-step procedure. In the first step, the true temporal mean of u_*^3 and the mean pressure correction, denoted as $F_{p,2}$, were computed using all the observations over the annual interval. In the second step, the calculation was repeated with the nighttime data only and the temporal averaging was approximated with the frequency-weighting method described above. The results are given in Fig. 10. This pattern factor was approximately 1.2 based on the two datasets. The annual pressure correction shown in Fig. 10 for this forest is lower than $40\,\mathrm{g\,C\,m^{-2}}$ given above because a fixed value of -2 was used for the stability factor F.

The results of the pressure correction estimate are summarized in Table 2. These numbers represent the annual total correction. They should be viewed as order-of-magnitude estimates only because of the uncertainties with regard to the u_* pattern factor and the stability factor, both of which may depend on site conditions. Despite the uncertainties, these results suggest the pressure fluctuations is a nonnegligible source of systematic bias in EC studies. Furthermore, the possibility exists that the bias errors are different for different ecotypes, therefore complicating the efforts of cross-site data synthesis.

The pressure corrections can affect the quality of gap-filling and NEE partitioning into its gross components. It is a common practice that nighttime NEE under low u_* conditions be replaced with

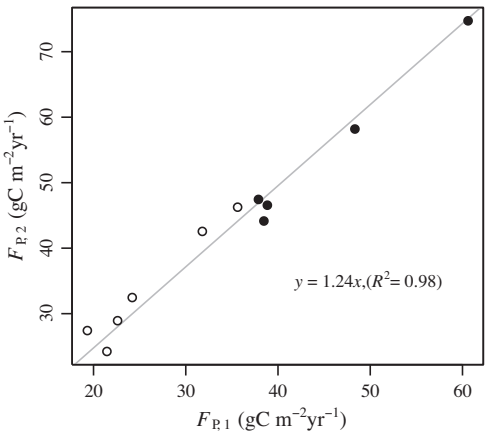

Fig. 10. Comparison of the annual cumulative pressure correction between the two methods described in the text. The assessment was made for this forest from 2005 to 2008 (denoted by ○) and for the Great Mountain Forest from 1999 to 2004 (Lee and Hu, 2002, denoted by ●).

observations made in high u_* conditions when static pressure fluctuations are large. Ignoring the pressure correction would bias the gap-filled ecosystem respiration towards lower values. It would also affect the estimate of gross primary production, causing it to be doubly overestimated because the pressure correction has opposite effects in the daytime and at night.

The present analysis is applicable to the open-path EC method. The open-path method is a commonplace in the long-term EC network, used at 60% of the AmeriFlux according to the site description on the FluxNet website (http://www.fluxnet.ornl.gov). So the pressure correction is clearly an important matter for the EC observation network. The density effect due to the pressure fluctuations is probably negligible on the closed-path EC. Massman (2004) argued that the sampling tube of the closed-path EC should have a negligible attenuation effect on pressure fluctuations and that other elements of the system may generate new pressure fluctuations but at frequencies that are too high to affect the CO_2 and w covariance calculations. According to Iberall (1950), there should be no lag in the pressure transmission through a tube containing an incompressible fluid. Since the CO_2 flux is computed with the CO_2 time series that is lagged by the time delay of the closed-path analyzer, to correct for the pressure effect one should also delay the static pressure oscilliations by the same amount in the computation of the w–p covariance in the correction term (Eq. (3)). Our data show that $\overline{w'p'}$ would decrease by 70% in magnitude if p' was delayed by 10 s and 90% if delayed by 20 s.

4. Summary

Our results indicate that canopy density had a negligible effect on the pressure spectral and cospectral distributions. In both the winter and summer seasons, the pressure power spectrum

Table 2
Annual pressure correction to the net CO_2 flux ($\mathrm{gC\,m^{-2}\,yr^{-1}}$).

Vegetation type[a]	Median[b]	Median[c]	Number of samples
Evergreen Needleleaf Forest (ENF)	32	65	8
Evergreen Broadleaf Forest (EBF)	23	47	6
Deciduous Broadleaf Forest (DBF)	41	83	12
Mixed Forest (MF)	40	81	11
Grassland (GRA)	1	11	7

[a] See Appendix A for papers from which the u_* data were obtained.
[b] Median value assuming $F = -2$ for forests and -0.2 for grassland.
[c] Median value assuming $F = -4$ for forests and -2 for grassland.

displayed a −3/2 slope in the inertial subrange. The peak w–p cospectral frequency appeared sensitive to thermal stratification.

The pressure flux ($\overline{w'p'}$) varied from nearly zero to −8 Pa m s^{-1} with an annual mean of −0.61 Pa m s^{-1}. The variations were largely controlled by friction velocity and air stability. The normalized flux F_p varied from −2 at neutral stability and became more negative as air became either unstable or stable. A nondimensional relationship, established for the normalized flux, can be used for gap-filling or assessing the pressure correction at sites where pressure measurements are not available.

Without the pressure correction, the EC method would underestimate the nighttime ecosystem respiration and overestimate the daytime photosynthetic carbon uptake. Over the experimental period, the annual cumulative correction amounted to 40 g C m^{-2} or roughly 20% of the annual net ecosystem production of this forest. Estimates based on the published data on friction velocity suggest that the pressure correction may also be important for other ecosystems in the long-term EC network (FluxNet).

Three issues deserve further investigation. First, arguments are presented to suggest that the pressure correction for the closed-path EC method should be negligible. This assessment is based on the unverified assertion that the pressure transmission through a sampling tube is instantaneous. Second, the limited published data suggest that the nondimensional relationship of the normalized pressure flux may be dependent on surface roughness. Of particular note is the large difference between F observed at our forest and that reported by McBean and Elliott (1975) for a grassland. Third, because of its bulkiness, the pressure sensor should be placed at some distance away from the sonic anemometer to avoid flow interference. How the sensor separation damps the pressure flux is not known. These issues will be investigated in our future field campaigns.

Acknowledgments

The research was funded by the National Natural Science Foundation of China (40930107, 40975071) and the Knowledge Innovation Program of the Chinese Academy of Sciences (KJCX2-YW-432). The first author thanks the KC Wong Education Foundation, Hong Kong for supporting his sabbatical visit to Yale University. The second author acknowledges a gift from the Rice Family Foundation that supports his collaborative research in China.

Appendix A. Literature used for Table 2

Evergreen Needleleaf Forest: Barr et al., 2006. Agricultural and Forest Meteorology, 140(1–4) 322–337; Griffis et al., 2003. Agricultural and Forest Meteorology, 117, 53–71; Hollinger et al., 1999. Global Change Biology, 5: 891–902; Humphreys et al., 2006. Agricultural and Forest Meteorology, 140: 6–22; Mammarella et al., 2007. Tellus Series B-Chemical and Physical Meteorology, 59: 900–909; Shibistova et al., 2002. Tellus Series B-Chemical and Physical Meteorology, 54: 568–589; Wen et al., 2005. Science in China Series D-Earth Sciences, 48: 63–73; Zha et al., 2004. Global Change Biology, 10: 1492–1503.

Evergreen Broadleaf Forest: Acevedo et al., 2009. Agricultural and Forest Meteorology, 149: 1–10; Hirano et al., 2007. Global Change Biology, 13: 412–425; Iwata et al., 2005. Agricultural and Forest Meteorology, 132: 305–314; Kosugi et al., 2008. Agricultural and Forest Meteorology, 148: 439–452; Loescher et al., 2003. Global Change Biology, 9: 396–412; Morgenstern et al., 2004. Agricultural and Forest Meteorology, 123: 201–219.

Deciduous Broadleaf Forest: Barr et al., 2006. Agricultural and Forest Meteorology, 140: 322–337; Bowling et al., 2001. Global Change Biology, 7: 127–145; Cook et al., 2004. Agricultural and Forest Meteorology, 126: 271–295; Granier et al., 2000. Functional Ecology, 14: 312–325; Hirata et al., 2007. Agricultural and Forest Meteorology, 147: 110–124; Ito et al., 2007. Tellus Series B-Chemical and Physical Meteorology, 59: 616–624; Knohl et al., 2003. Agricultural and Forest Meteorology, 118: 151–167; Oren et al., 2006. Global Change Biology, 12: 883–896; Pilegaard et al., 2001. Agricultural and Forest Meteorology, 107: 29–41; Paw U et al., 2004. Ecosystems, 7: 513–524; Wharton et al., 2009. Agricultural and Forest Meteorology, 149: 1477–1490.

Mixed Forest: Carrara et al., 2003. Agricultural and Forest Meteorology, 119: 209–227; Davis et al., 2003. Global Change Biology, 9: 1278–1293; Haszpra et al., 2005. Agricultural and Forest Meteorology, 132: 58–77; Hollinger et al., 1999. Global Change Biology, 5: 891–902; Marcolla et al., 2005. Agricultural and Forest Meteorology, 130: 193–206; McCaughey et al., 2006. Agricultural and Forest Meteorology, 140: 79–96; Monson et al., 2002. Global Change Biology, 8: 459–478; Pilegaard et al., 2001. Agricultural and Forest Meteorology, 107: 29–41; Schmid et al., 2000. Agricultural and Forest Meteorology, 103: 357–374; Teklemariam et al., 2009. Agricultural and Forest Meteorology, 149: 2040–2053; Zhang et al., 2006. Agricultural and Forest Meteorology, 137: 150–165.

Grassland: Flanagan et al., 2002. Global Change Biology, 8: 599–615; Myklebust et al., 2008. Agricultural and Forest Meteorology, 148: 1894–1907; Pattey et al., 2002. Agricultural and Forest Meteorology, 113: 145–158; Sims and Bradford, 2001. Agricultural and Forest Meteorology, 109: 117–134; Stoy et al., 2006. Agricultural and Forest Meteorology, 141: 2–18; Wohlfahrt et al., 2005. Agricultural and Forest Meteorology, 128: 141–162; Xu and Baldocchi, 2004. Agricultural and Forest Meteorology, 123: 79–96.

References

Albertson, J.D., Katul, G.G., Parlange, M.B., Eichinger, W.E., 1998. Spectral scaling of static pressure fluctuations in the atmospheric surface layer: the interaction between large and small scales. Physics of Fluids 10 (7), 1725–1732.

Aubinet, M., 2008. Eddy covariance CO_2 flux measurements in nocturnal conditions: an analysis of the problem. Ecological Applications 18 (6), 1368–1378.

Aubinet, M., Heinesch, B., Yernaux, M., 2003. Horizontal and vertical CO_2 advection in a sloping forest. Boundary-Layer Meteorology 108 (3), 397–417.

Baldocchi, D.D., 2003. Assessing the eddy covariance technique for evaluating carbon dioxide exchange rates of ecosystems: past, present and future. Global Change Biology 9 (4), 479–492.

Baldocchi, D.D., Finnigan, J., Wilson, K., Paw U, K.T., Falge, E., 2000. On measuring net ecosystem carbon exchange over tall vegetation on complex terrain. Boundary-Layer Meteorology 96 (1–2), 257–291.

Barthlott, C., Drobinski, P., Fesquet, C., Dubos, T., Pietras, C., 2007. Long-term study of coherent structures in the atmospheric surface layer. Boundary-Layer Meteorology 125, 1–24.

Berger, B.W., Davis, K.J., Yi, C., Bakwin, P.S., Zhao, C.L., 2001. Long-term carbon dioxide fluxes from a very tall tower in a northern forest: flux measurement methodology. Journal of Atmospheric and Oceanic Technology 18 (4), 529–542.

Blake, W.K., 1970. Turbulent boundary layer wall pressure fluctuations on smooth and rough walls. Journal of Fluid Mechanics 44 (4), 637–660.

Canavero, F.G., Einaudi, F., 1987. Time and space variability of spectral estimates of atmospheric pressure. Journal of the Atmospheric Sciences 44 (12), 1589–1604.

Conklin, P.S., 1994. Turbulent Wind, Temperature and Pressure in a Mature Hardwood Canopy. Ph.D. Thesis. Duke University, 116 pp.

Elliott, J.A., 1972. Microscale pressure fluctuations measured within lower atmospheric boundary-layer. Journal of Fluid Mechanics 53 (4), 351–383.

Fitzmaurice, L., Shaw, R.H., Kyaw, T.P.U., Patton, E.G., 2004. Three-dimensional scalar microfront systems in a large-eddy simulation of vegetation canopy flow. Boundary-Layer Meteorology 112 (1), 107–127.

Foufoula-Georgiou, E., Kumar, P., 1994. Wavelets in Geophysics Volume 4 (Wavelet Analysis and Its Applications). Academic Press, San Diego.

Gao, W., Shaw, R.H., Paw, K.T., 1992. Conditional analysis of temperature and humidity microfronts and ejection sweep motions within and above a deciduous forest. Boundary-Layer Meteorology 59 (1–2), 35–57.

Gotoh, T., Rogallo, R.S., 1999. Intermittency and scaling of pressure at small scales in forced isotropic turbulence. Journal of Fluid Mechanics 396, 257–285.

Goulden, M.L., Miller, S.D, da Rocha, H.R., 2006. Nocturnal cold air drainage and pooling in a tropical forest. Journal of Geophysical Research-Atmospheres 111, D08S04, doi:10.1029/2005JD006037.

Grace, J., Malhi, Y., Lloyd, J., Mcintyre, J., Miranda, A.C., Meir, P., Miranda, H.S., 1996. The use of eddy covariance to infer the net carbon dioxide uptake of Brazilian rain forest. Global Change Biology 2 (3), 209–217.

Grachev, A.I., Mordukhovich, M.I., 1988. Spectrum of pressure fluctuations in the atmospheric ground layer Izvestiya. Atmospheric and Oceanic Physics 24 (2), 159–160.
Iberall, A.S., 1950. Attenuation of oscillatory pressures in instrument lines. Journal of Research of the National Bureau of Standards 45 (1), 85–108.
Kaimal, J.C., Finnigan, J.J., 1994. Atmospheric Boundary Layer Flows: Their Structure and Measurement. Oxford University Press, New York.
Kimball, B.A., Lemon, E.R., 1970. Spectra of air pressure fluctuations at soil surface. Journal of Geophysical Research 75 (33), 6771–6777.
Lee, X.H., 1997. Gravity waves in a forest: a linear analysis. Journal of the Atmospheric Sciences 54 (21), 2574–2585.
Lee, X.H., 1998. On micrometeorological observations of surface-air exchange over tall vegetation. Agricultural and Forest Meteorology 91 (1–2), 39–49.
Lee, X.H., Hu, X.Z., 2002. Forest-air fluxes of carbon, water and energy over non-flat terrain. Boundary-Layer Meteorology 103 (2), 277–301.
Lee, X.H., Shaw, R.H., Black, T.A., 1994. Modeling the effect of mean pressure gradient on the mean flow within forests. Agricultural and Forest Meteorology 68 (3–4), 201–212.
Lu, C.H., Fitzjarrald, D.R., 1994. Seasonal and diurnal variations of coherent structures over a deciduous forest. Boundary-Layer Meteorology 69 (1–2), 43–69.
Mahrt, L., Gibson, W., 1992. Flux decomposition into coherent structures. Boundary-Layer Meteorology 60 (1–2), 143–168.
Maitani, T., Seo, T., 1985. Estimates of velocity–pressure and velocity–pressure gradient interactions in the surface-layer over plant canopies. Boundary-Layer Meteorology 33 (1), 51–60.
Maraun, D., 2006. What Can We Learn from Climate Data? Methods for Fluctuation, Time/Scale and Phase Analysis. Ph.D. Thesis. University of Potsdam.
Massman, W.J., 2004. In: Lee, X., Massman, W., Law, B. (Eds.), Concerning the Measurements of Atmospheric Trace Gas Fluxes with open- and Closed-path Eddy Covariance system: the WPL Terms and Spectral Attenuation in Handbook of Micrometeorology: A Guide for Surface Flux Measurement and Analysis. Kluwer Academic Publishers, Dordrecht, pp. 133–160.
Massman, W.J., Lee, X., 2002. Eddy covariance flux corrections and uncertainties in long-term studies of carbon and energy exchanges. Agricultural and Forest Meteorology 113 (1–4), 121–144.
McBean, G.A., Elliott, J.A., 1975. Vertical transports of kinetic-energy by turbulence and pressure in boundary-layer. Journal of the Atmospheric Sciences 32 (4), 753–766.
McBean, G.A., Elliott, J.A., 1978. Energy budgets of turbulent velocity components and velocity–pressure gradient interactions. Journal of the Atmospheric Sciences 35 (10), 1890–1899.
Muggeo, V.M.R., 2003. Estimating regression models with unknown break-points. Statistics in Medicine 22 (19), 3055–3071.
Paw, U.K.T., Baldocchi, D.D., Meyers, T.P., Wilson, K.B., 2000. Correction of Eddy-covariance measurements incorporating both advective effects and density fluxes. Boundary-Layer Meteorology 97 (3), 487–511.
R Development Core Team, 2009. R: A Language and Environment for Statistical Computing. R Foundation for Statistical Computing, Vienna, Austria. ISBN: 3-900051-07-0, http://www.R-project.org.
Raupach, M.R., Finnigan, J.J., Brunet, Y., 1996. Coherent eddies and turbulence in vegetation canopies: the mixing-layer analogy. Boundary-Layer Meteorology 78 (3–4), 351–382.
Robertson, P., 1972. A direction-insensitive static head sensor. Journal of Physics E: Scientific Instruments 5 (11), 1080–1082.
Shaw, R.H., Paw, U.K.T., Zhang, X.J., Gao, W., Den Hartog, G., Neumann, H.H., 1990. Retrieval of turbulent pressure-fluctuations at the ground surface beneath a forest. Boundary-Layer Meteorology 50 (1–4), 319–338.
Sigmon, J.T., Knoerr, K.R., Shaughnessy, E.J., 1983. Microscale pressure-fluctuations in a mature deciduous forest. Boundary-Layer Meteorology 27 (4), 345–358.
Staebler, R.M., Fitzjarrald, D.R., 2004. Observing subcanopy CO_2 advection. Agricultural and Forest Meteorology 122 (3–4), 139–156.
Thomas, C., Foken, T., 2007. Flux contribution of coherent structures and its implications for the exchange of energy and matter in a tall spruce canopy. Boundary-Layer Meteorology 123 (2), 317–337.
Webb, E.K., Pearman, G.I., Leuning, R., 1980. Correction of flux measurements for density effects due to heat and water-vapor transfer. Quarterly Journal of the Royal Meteorological Society 106 (447), 85–100.
Wilczak, J.M., Businger, J.A., 1984. Large-scale eddies in the unstably stratified atmospheric surface layer part II: turbulent pressure fluctuations and the budgets of heat flux, stress and turbulent kinetic energy. Journal of the Atmospheric Sciences 41 (24), 3551–3567.
Wilczak, J.M., Edson, J.B., Hgstrup, J., Hara, T., 1999. The budget of turbulent kinetic energy in the marine atmospheric surface layer. In: Geernaert, G.L. (Ed.), Air–Sea Exchange: Physics, Chemistry, and Dynamics. Kluwer Academic Publishers, Dordrecht The Netherlands, pp. 153C173.
Zhang, J., Han, S., Yu, G., 2006a. Seasonal variation in carbon dioxide exchange over a 200-year-old Chinese broad-leaved Korean pine mixed forest. Agricultural and Forest Meteorology 137 (3–4), 150–165.
Zhang, J., Yu, G., Han, S., Guan, D., Sun, X., 2006b. Seasonal and annual variation of CO_2 flux above a broadleaved Korean pine mixed forest. Science in China Series D-Earth Sciences 49, 63–73.
Zhuang, Y., Amiro, B.D., 1994. Pressure fluctuations during coherent motions and their effects on the budgets of turbulent kinetic energy and momentum flux within a forest canopy. Journal of Applied Meteorology 33 (6), 704–711.